PHYSICAL REVIEW A **87**, 041403(R) (2013)

Coulomb effects in photon-momentum partitioning during atomic ionization by intense linearly polarized light

J. Liu,[1,2] Q. Z. Xia,[1] J. F. Tao,[1] and L. B. Fu[1,2]

[1]*National Laboratory of Science and Technology on Computational Physics, Institute of Applied Physics and Computational Mathematics, Beijing 100088, China*

[2]*HEDPS, Center for Applied Physics and Technology, Peking University, Beijing 100084, China*

(Received 10 October 2012; published 22 April 2013)

Partitioning of photon momenta between the ion and electron in photoionization and the involved subcycle dynamics are investigated using an extended semiclassical model, where momentum transfer from the photon to the electron-ion system via the (magnetic) Lorentz force is taken into account. It is found that in both the tunneling and rescattering processes, Coulomb attraction between the ion and electron plays a role in the momentum partitioning. The effect is especially important for linearly polarized light since the photons that lift the electron out of the bound state do not always contribute to the forward ion momentum. The present results can have important implications in the generation of terahertz radiation and the calibration of tunnel exit by measuring final ion longitudinal momentum.

DOI: 10.1103/PhysRevA.87.041403 PACS number(s): 32.80.Rm, 42.50.Hz, 33.80.Rv

Introduction. In light-atom interactions, besides the often-invoked photon energy and angular momentum [1,2], another property, namely, the linear photon momentum, is seldom considered. This is partly because the linear (hereafter omitted for simplicity) momentum of a visible photon is extremely small. On the other hand, an intense laser pulse contains many photons, and their combined momenta can give rise to macroscopic effects. The latter include radiation pressure [3,4], which has important applications, such as manipulation of cold atoms [5], acceleration of particles [6,7], generation of terahertz radiation [8–11], etc.

An intriguing question associated with photon-momentum transfer in strong-field atomic ionization is, how are the photon momenta partitioned between the electron and ion? The question had not been addressed until a recent exquisite experiment [12], which attempted to quantify the effect of the radiation pressure on the individual electrons in multiphoton ionization of circularly polarized (CP) laser light. In the classical [12] interpretation of the observed results, the ion and electron from the ionization are assumed to move independently in the laser fields, with the Coulomb interaction between them ignored. However, in the linearly polarized (LP) light field, Coulomb interaction is of great importance and can lead to Coulomb focusing [13], recapture or rescattering [14,15], low-energy surprise [16], interference carpet structure [17], partial atomic stabilization [18], etc. Considering that photon-momentum partition between the ion and electron can occur in both the ionization and posttunneling scattering (i.e., rescattering) processes, we can expect that Coulomb attraction also plays a role in photon-momentum partitioning.

In this Rapid Communication, we propose a semiclassical model to account for photon-momentum partitioning between the ion and electron in atomic ionization by intense laser light. The model includes tunneling ionization and the classical dynamics of the valence electron and ion in the combined laser and Coulomb fields. It can thus also be used to investigate the subcycle dynamics of the photon-momentum partitioning. Our results show that Coulomb attraction between the ion and electron can affect photon-momentum transfer in both the tunneling and posttunneling scattering processes, even for CP light. For LP light, momentum transfer to the ion is found to be greatly increased due to the rescattering, so that the photons that lift the electron from the bound to the continuum state do not contribute to the forward momentum of the ion. This conclusion differs from that of earlier works [12,19]. The underlying microscopic trajectory configurations are studied, and important implications are discussed.

Semiclassical model. The proposed semiclassical model accounts for the full ion and electron dynamics, including tunneling ionization and scattering of electrons in the combined Coulomb and electromagnetic fields. The tunneling electron (released at a distance r_0 from the ion) has zero parallel velocity and a Gaussian transverse (with respect to the direction of instantaneous electric field) velocity distribution [20]: $f(v_\perp) = \exp[-\sqrt{2I_p}v_\perp^2/|\epsilon(t)|]$, in which I_p is the atomic ionization potential, $\epsilon(t)$ is the laser electric field, and atomic units are used throughout. In order to account for the motion of the ion core, we have assigned its initial momentum according to $p^e_{x0} + p^i_{x0} = p^e_{y0} + p^i_{y0} = 0$ and $p^e_{z0} + p^i_{z0} = (E^e_{k0} - 1/r_0 + I_p)/c$; here electron kinetic energy $E^e_{k0} = v_\perp^2/2$, $\vec{p}^{\,e}_0$ and $\vec{p}^{\,i}_0$ are the initial momentum of the electron and ion, respectively, c is the vacuum light speed, and z is the propagation direction. Consequently, the electron and ion move in the combined electromagnetic and Coulomb fields and are governed by Newton's equations [21,22].

The electric field is given by

$$\vec{E} = \frac{\epsilon_0}{\sqrt{\chi^2+1}}\exp\left[-\frac{2\ln 2}{c^2\tau^2}(z-ct)^2\right][\cos(\omega t - kz)\vec{e}_x + \chi\sin(\omega t - kz)\vec{e}_y],$$

where χ is the ellipticity. The magnetic field is given by $\vec{e}_z \times \vec{E}/c$. For each t_0 we can calculate the electron tunneling point and the electron velocity $v_\perp$ perpendicular to the instantaneous electric field, and we attribute a rate $w(t_0)f(v_\perp)$ to the event [22]. We then take the average over all velocities and tunneling phases to obtain the physical quantities of interest, such as momentum gain and loss of the electron and ion.

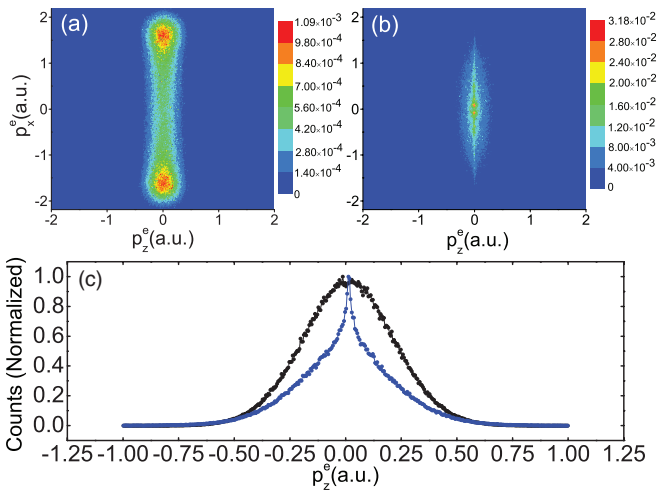

FIG. 1. (Color online) Simulated electron-momentum spectrum for Ne atom ionization by 800 nm, 8×10^{14} W cm^{-2} lasers of (a) CP and (b) LP polarization. (c) Simulated Ne photoelectron-momentum distribution along the propagation direction. Black [blue (gray)] dotted line: results for the CP (LP) light.

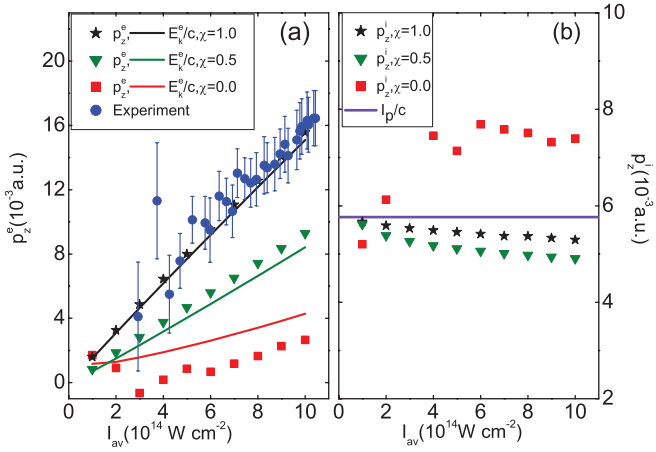

FIG. 2. (Color online) (a) Average electron momentum along the propagation (z) direction as a function of the laser intensity. The points denote the simulated average electron momentum. The lines denote the simulated average electron kinetic energy E_k^e divided by the vacuum light speed c. Blue circles: experimental data from Ref. [12]. Black stars: results for CP light with $\chi = 1$. Green downward triangles: results of elliptically polarized light with $\chi = 0.5$. Red squares: results for LP light with $\chi = 0$. (b) Average ion momentum along the laser propagation direction. The violet horizontal line is for $p_z^i = I_p/c$.

Model calculation. We apply the model to a Ne atom with the ionization potential parameters $I_p = 0.79$ a.u.. The screening potential is introduced to depict the interaction between the valence electron and the ion, i.e., $V_s(\vec{r}_i - \vec{r}_e) = -[(Z-1)s(|\vec{r}_i - \vec{r}_e|) + 1]/|\vec{r}_i - \vec{r}_e|$, where $s(r) = [H(e^{r/d} - 1) + 1]^{-1}$, Z is the nuclear charge, and H and d are two atomic parameters [23]. The wavelength of laser light is 800 nm, and the pulse duration is $\tau = 15$ fs [12]. In our simulations, Newton's equations are solved using a fourth order Runge-Kutta numerical algorithm. More than 1 000 000 classical trajectories are used, and numerical convergence has been tested by doubling the number of trajectories.

We present in Fig. 1(a) [Fig. 1(b)] and with the black [blue (gray)] dotted line in Fig. 1(c) the results for CP (LP) light. One can see two bright spots in the spectrum of Fig. 1(a) but not in Fig. 1(b), which is due to the distinct symmetry of CP and LP fields. Moreover, the blue dotted line in Fig. 1(c) clearly reveals Coulomb focusing [13]. Taking the average over the distributions in Fig. 1(c), we find that for both CP and LP lights the electron can gain a net momentum along the laser propagation direction, i.e., the average longitudinal momentum $\langle p_z \rangle > 0$.

Figure 2 shows the electron and ion average momentum (i.e., net momentum gain) as a function of the light intensity. From Fig. 2(a), we see that our model calculations on the electron momentum gains in CP fields are in good agreement with experimental observations [12]. The net electron momentum was also be obtained by the quantum scattering matrix without considering the ion's motion [19]. In contrast to the quantum treatment, in our model, the electron gains or loses longitudinal momentum on its way out of the laser beam, which is automatically and fully included. Our simulations at the same time are able to trace the motions of ions and generate the ion-momentum gains, as shown in Fig. 2(b). For CP fields, the average ion momentum p_z^i fairly follows the I_p/c dependence with small deviations that depend on the laser intensity. However, for the LP case, we find that the net ion momentum exhibits a sudden increment around 2×10^{14} W cm^{-2}, above which the simulation results deviate from the assertion [12,19] $p_z^i = I_p/c$ by up to 30%. We have also checked the momentum-energy relation $p_z^e + p_z^i = (E_k^e + I_p)/c$ from our simulation. Note that, even with the inclusion of the Coulomb interaction, our model does not produce negative [12] average electron momentum at low intensities.

The "simple-man model" [24] of atomic ionization invokes the relation $p_z^i = I_p/c$ or $p_z^e = E_k^e/c$, which assumes that the electron is tunneled out with zero initial velocity at the origin and then executes a quiver motion in the light wave. In the tunneling process, the electron and ion are tightly bound, and the part of the longitudinal momentum I_p/c corresponding to the photon momentum necessary to overcome the ionization energy must be transferred to the center of mass of the electron-ion system, i.e., $p_z^i = I_p/c$. In the posttunneling process, the electron absorbs excessive photon energy and momentum, so that one obtains $p_z^e = E_k^e/c$. This simple picture ignores the Coulomb attraction between the ion and electron in both the tunneling and posttunneling scattering processes and therefore cannot account for the above simulations.

Coulomb effects. Tunneling ionization can be described by an effective potential in parabolic coordinates [25]. The tunneling electron is emitted along the direction of instantaneous electric field at a nonzero distance of r_0 from the ion [26]. The distance depends on the field strength and the ionization potential and can be approximated by $r_0 \simeq I_p/\epsilon$ [22,27], where $\epsilon = \epsilon_0 \exp[-2\ln 2(t_0^2/\tau^2)]$ is the electric field at t_0 in the plane $z = 0$. In addition, the tunneling electron has a Gaussian transverse velocity distribution of $v_\perp$. That is, before tunneling, the electron-ion system has a bound energy of $-I_p$, and after tunneling, the system energy is $v_\perp^2/2 - 1/r_0$ [28], so

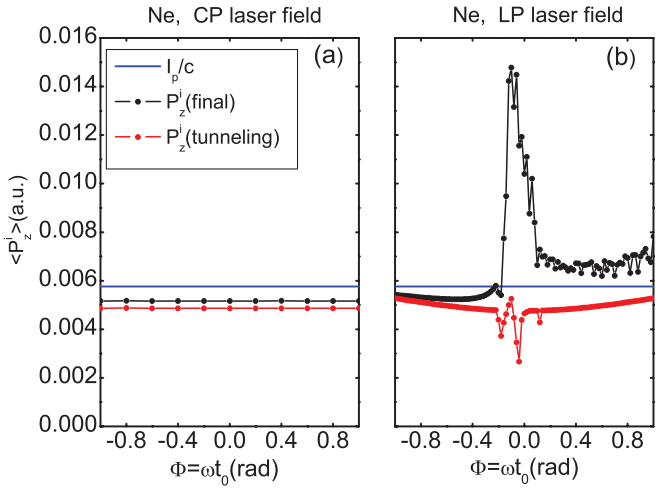

FIG. 3. (Color online) The average ion momentum as a function of the initial laser phase for Ne at 800 nm: (a) 10×10^{14} W cm^{-2} for CP fields and (b) 16×10^{14} W cm^{-2} for LP fields. Red (light gray) line: the ion momentum just after tunneling. Black line: the simulated final average ion momentum. The horizontal blue (dark gray) line indicates $p_z^i = I_p/c$.

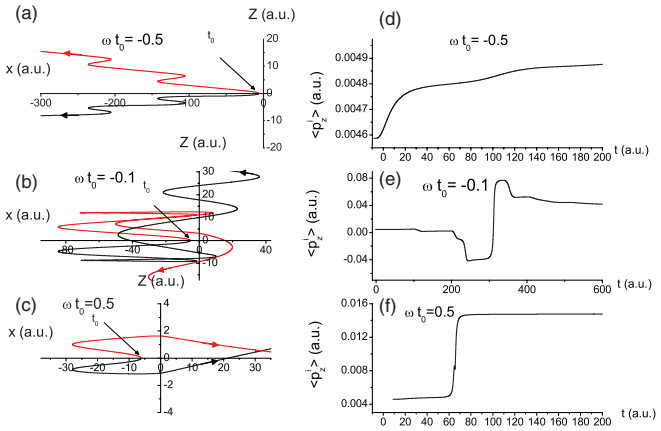

FIG. 4. (Color online) Typical electron trajectories with different tunneling phases of (a)−0.5, (b) −0.1, and (c) 0.5. For each phase, a pair of trajectories is plotted with the initial opposite velocities. (d)–(f) The time-resolved net ion momentum averaged over the trajectory pairs corresponding to (a)–(c), respectively.

that the system energy increment in the tunneling process is $v_\perp^2/2 - 1/r_0 + I_p$. Here we have ignored the kinetic energy of the ion. The photon momentum should be shared between the ion and electron, that is, $p_{z0}^e + p_{z0}^i = (v_\perp^2/2 - 1/r_0 + I_p)/c$. Taking the average over the ensemble of all transverse velocities and noting that $\langle p_{z0}^e \rangle = 0$, $\langle v_\perp^2 \rangle = \epsilon/\sqrt{2I_p}$, we get $\langle p_{z0}^i \rangle = (\epsilon/2\sqrt{2I_p} - \epsilon/I_p + I_p)/c$. Figure 3 shows the initial-phase (ωt_0) dependence of the average ion momentum [red (light gray) curves] just after tunneling for CP light and LP light, respectively. In contrast to the simple-man model, the net longitudinal momentum acquired by the ion in the tunneling process deviates from I_p/c by a quantity of order ϵ_0 for both LP and CP laser fields. The small fluctuations near zero phase for the LP case are due to the events when the electron tunnels without ionization [29,30].

The Coulomb attraction between the ion and electron is also involved in the posttunneling scattering process. In CP laser fields, the tunneling electron has a velocity proportional to the instantaneous electric field strength and is directed perpendicular to the instantaneous polarized field direction. The electron spirals away from its parent ion without returning [27]. Thus, the ion can only acquire longitudinal momentum from a limited number of photons [Fig. 3(a)]. In the LP fields, on the other hand, the electron in a certain initial phase window can revisit its parent ion [14,22], leading to the repartitioning of the photon momentum between the ion and electron. The momentum transfer to the ion is found to be significantly increased [Fig. 3(b)].

The scenario given above is helpful for understanding the observed sudden change of the net ion momentum at the laser intensity 2×10^{14} W cm^{-2} in Fig. 2(b). The tunneling electron is released at a distance I_p/ϵ_0 from the core ion. The characteristic displacement of the quiver motion of the tunneling electron in the electric field is ϵ_0/ω^2. With the decrease of the laser intensity, the quiver length decreases while the exit distance increases. When the quiver length is smaller than the exit distance, the electron will have little chance to recollide with the ion. The corresponding threshold intensity is $\epsilon_0^{th} \simeq \omega\sqrt{I_p}$, which approximates to 1×10^{14} W cm^{-2}, comparable with the numerical results. The deviation is due to the electron traverse velocity, which might decrease the collision possibility and increase the threshold field.

Subcycle dynamics. Coulomb interaction affects photon-momentum partitioning in both the tunneling and posttunneling scattering processes. For LP light, the Coulomb-interaction modified scattering is more complex and crucial in determining the final momentum partitioning. In the following, we shall investigate in more detail the subcycle dynamics of the photon-momentum transfer in the posttunneling scattering, especially for the LP fields.

Figures 4(a)–4(c) show three pairs of typical electron trajectories corresponding to three different initial phase regimes, i.e., $\omega t_0 < -0.2$, $-0.2 < \omega t_0 < 0.1$, and $\omega t_0 > 0.1$, respectively. The trajectories are projected on the plane of the polarization direction (x) and the light propagation direction (z). For each pair of electron orbits, the initial velocities are opposite but have the same amplitude. Note that the two orbits are asymmetric with respect to the x axis because the photons can push the electrons forward along the propagation direction. These electrons can in turn pull the ion core forward along the positive z direction through the Coulomb attraction force. Figure 4(a) shows that the electrons move out directly, with some quiver oscillations. Figure 4(c) shows the electron trajectories for $\omega t_0 > 0.1$, where the electron can return to the neighborhood of the ion core once. We present in Figures 4(d)–4(f) the time-resolved net ion momentum. The behaviors for the initial phases $\omega t_0 = -0.5$ and 0.5 are relatively simple: both show an almost monotonous increase initially and then show saturation when the electrons are far away from the ion. The increase for $\omega t_0 = 0.5$ is larger because, in this case, the net ion momentum gain mainly emerges when the electrons return to the ion, and, at that moment, the electrons are closer to the ion and can pull the ion forward more strongly.

When the initial phase is in the regime $-0.2 < \omega t_0 < 0.1$, the posttunneling electron trajectories are complex. Figure 4(b) shows that multiple returns and collisions with the ion core can occur. We see that Coulomb attraction between the returning electrons and the ion core at collisions leads to a dramatic change in the orbits, which in turn modifies the momentum transfer. For $\omega t_0 = -0.1$, the net ion momentum first decreases, then increases, and finally decreases with some step structures in between. The electrons can long-term entangle with the ion, bounded by Coulomb attraction. At this stage, the photon prefers to transfer its momentum to the ion rather than the electron, and the ion can obtains a large amount of longitudinal momenta on average. The long-term trapped orbits are responsible for the peak structure near zero phase in Fig. 3(b). It is of interest to point out that if the electron tunnels at $\omega t_0 \sim -0.1$, the final ion momentum is very sensitive to the electron's initial velocity, indicating the onset of chaos [22,31]. Chaotic orbits have been shown to account for the higher above-threshold energy spectra [22], high-order-harmonic generation [32], and double ionization [27,33]. It is evident that chaos is involved in the photon momentum partitioning.

In summary, we found that Coulomb interaction between the electron and ion is important in the photon-momentum partitioning. Our theory provides insight into the recent experiment and predicts for Ne atoms that the momentum transfers to the ion will be evidently increased for the linearly polarized laser fields [34]. There are some important implications of the results. First, the photon-momentum transfer to the electron has been invoked to account for terahertz generation in filaments. The results here are important for concurrent models of the generation of terahertz radiation in filaments [11]. Second, our results provide a mechanism to transfer the photon momentum to the ion in the tunneling ionization. We quantify the effect and associate it explicitly with the tunnel exit, thus providing a possible way to calibrate the tunnel exit through the measurement of the net ion longitudinal momentum, which is of great concern [26] and has implications in attosecond angular streaking [35].

Acknowledgments. We are grateful to Dr. P. B. Corkum and Dr. M. Y. Yu for stimulating discussions. This work is supported by the NFRP (Grants No. 2011CB921503, No. 2013CBA01502, and No. 2013CB834100) and the NNSF of China (Grants No. 91021021 and No. 11274051).

[1] *Atoms in Intense Laser Fields*, edited by M. Gavrila (Academic, Boston, 1992).

[2] *Strong Field Laser Physics*, edited by T. Brabec (Springer, New York, 2009).

[3] G. Marx, Nature (London) **211**, 22 (1966).

[4] S. Gigan, H. R. Böhm, M. Paternostro, F. Blaser, G. Langer, J. B. Hertzberg, K. C. Schwab, D. Bäuerle, M. Aspelmeyer, and A. Zeilinger, Nature (London) **444**, 67 (2006).

[5] C. Chin, R. Grimm, P. Julienne, and E. Tiesinga, Rev. Mod. Phys. **82**, 1225 (2010).

[6] U. Eichmann *et al*., Nature (London) **461**, 1261 (2009); Q. Z. Xia, L. B. Fu, and J. Liu, Phys. Rev. A **87**, 033404 (2013).

[7] M. Hegelich *et al*., Phys. Rev. Lett. **89**, 085002 (2002).

[8] C. D. Amico *et al*., New J. Phys. **10**, 013015 (2008).

[9] P. Sprangle, J. R. Penano, B. Hafizi, and C. A. Kapetanakos, Phys. Rev. E **69**, 066415 (2004).

[10] C. C. Cheng, E. M. Wright, and J. V. Moloney, Phys. Rev. Lett. **87**, 213001 (2001).

[11] B. Zhou, A. Houard, Y. Liu, B. Prade, A. Mysyrowicz, A. Couairon, P. Mora, C. Smeenk, L. Arissian, and P. Corkum, Phys. Rev. Lett. **106**, 255002 (2011).

[12] C. T. L. Smeenk, L. Arissian, B. Zhou, A. Mysyrowicz, D. M. Villeneuve, A. Staudte, and P. B. Corkum, Phys. Rev. Lett. **106**, 193002 (2011).

[13] T. Brabec, M. Y. Ivanov, and P. B. Corkum, Phys. Rev. A **54**, R2551 (1996).

[14] P. B. Corkum, Phys. Today **64**(3), 36 (2011); Phys. Rev. Lett. **71**, 1994 (1993).

[15] W. Becker and H. Rottke, Contemp. Phys. **49**, 199 (2008).

[16] C. I. Blaga *et al*., Nat. Phys. **5**, 335 (2009); W. Quan *et al*., Phys. Rev. Lett. **103**, 093001 (2009).

[17] Ph. A. Korneev, S. V. Popruzhenko, S. P. Goreslavski, T.-M. Yan, D. Bauer, W. Becker *et al*., Phys. Rev. Lett. **108**, 223601 (2012).

[18] H. Liu *et al*., Phys. Rev. Lett. **109**, 093001 (2012).

[19] A. S. Titi and G. W. F. Drake, Phys. Rev. A. **85**, 041404(R) (2012).

[20] N. B. Delone and V. P. Krainov, J. Opt. Soc. Am. B **8**, 1207 (1991).

[21] The classical dynamics is a feasible way to understand complex strong-field ionization; see X. Wang and J. H. Eberly, Phys. Rev. Lett. **103**, 103007 (2009); **105**, 083001 (2010); Phys. Rev. A **86**, 013421 (2012).

[22] B. Hu, J. Liu, and S. G. Chen, Phys. Lett. A **236**, 533 (1997).

[23] P. P. Szydlik and A. E. S. Green, Phys. Rev. A **9**, 1885 (1974).

[24] H. B. van Linden van den Heuvell and H. G. Muller, in *Multiphoton Processes*, edited by S. J. Smith and P. L. Knight (Cambridge University Press, Cambridge, 1988); T. F. Gallagher, Phys. Rev. Lett. **61**, 2304 (1988); P. B. Corkum, N. H. Burnett, and F. Brunel, *ibid*. **62**, 1259 (1989).

[25] L. D. Landau and E. M. Lifshitz, *Quantum Mechanics* (Pergamon, New York, 1977).

[26] D. D. Hickstein, P. Ranitovic, S. Witte, X. M. Tong *et al*., Phys. Rev. Lett. **109**, 073004 (2012).

[27] L. B. Fu, G. G. Xin, D. F. Ye, and J. Liu, Phys. Rev. Lett. **108**, 103601 (2012).

[28] Because $r_0 \gg 1$ a.u., the screening potential reduces to the Coulomb type, so that potential energy can be approximated by $1/r_0$ at this distance.

[29] T. Nubbemeyer, K. Gorling, A. Saenz, U. Eichmann, and W. Sandner, Phys. Rev. Lett. **101**, 233001 (2008).

[30] K. Huang, Q. Xia, and L.-B. Fu, Phys. Rev. A **87**, 033415 (2013).

[31] J. Liu, S. G. Chen, and B. Hu, Acta Phys. Sin. (Overseas Edn) **7**, 89 (1998).

[32] G. van de Sand and J. M. Rost, Phys. Rev. Lett. **83**, 524 (1999).

[33] F. Mauger, C. Chandre, and T. Uzer, Phys. Rev. Lett. **102**, 173002 (2009).

[34] The net ion momentum might be either increased or reduced in the rescattering process of LP laser fields, sensitively depending on the core potentials that vary with atomic species. For atoms with a smaller nuclear charge number such as helium, we find that net ion momentum might be reduced compared to I_p/c. Details will be presented elsewhere.

[35] A. N. Pfeiffer, C. Cirelli, M. Smolarski, D. Dimitrovski, M. Abusamha, L. B. Madsen, and U. Keller, Nat. Phys. **8**, 76 (2012).